Carbohydrate Polymers 99 (2014) 700–709

Contents lists available at ScienceDirect

Carbohydrate Polymers

journal homepage: www.elsevier.com/locate/carbpol

Osteogenesis induction of periodontal ligament cells onto bone morphogenic protein-2 immobilized PCL fibers

Sung Eun Kim[a,1], Young-Pil Yun[a,1], Yun-Kyung Han[b], Deok-Won Lee[b], Joo-Young Ohe[b], Baek-Soo Lee[b], Hae-Ryong Song[a], Kyeongsoon Park[c,**], Byung-Joon Choi[b,*]

[a] Department of Orthopedic Surgery & Rare Diseases Institute, Korea University Medical Center, Guro Hospital, #148, Gurodong-ro, Guro-gu, Seoul 152-703, Republic of Korea
[b] Department of Oral and Maxillofacial Surgery, School of Dentistry, Kyung Hee University, #1 Hoegi-dong, Dongdaemun-gu 130-701, Republic of Korea
[c] Division of Bioimaging, Chuncheon Center, Korea Basic Science Institute, 192-1 Hyoja 2-dong, Chuncheon, Gangwon-do 200-701, Republic of Korea

ARTICLE INFO

Article history:
Received 30 January 2013
Received in revised form 28 July 2013
Accepted 20 August 2013
Available online 28 August 2013

Keywords:
Periodontal ligament cells (PDLCs)
Bone morphogenic protein-2 (BMP-2)
PCL fiber
Osteogenesis induction

ABSTRACT

The purpose of this study was to develop bone morphogenic protein-2 (BMP-2) immobilized PCL fibers to induce osteogenic differentiation of periodontal ligament cells (PDLCs). The PCL fiber surface was modified with heparin-dopamine (Hep-DOPA) (Hep-PCL) and further immobilized with BMP-2 (BMP-2/Hep-PCL). PCL fibers and surface-modified PCL fibers (Hep-PCL and BMP-2/Hep-PCL) were characterized by X-ray photoelectron spectroscopy (XPS) and contact angle. Osteogenic differentiation of PDLCs was demonstrated by alkaline phosphatase (ALP) activity, calcium deposition, and gene expression. The results of XPS and contact angle revealed that Hep-DOPA and BMP-2 were successfully immobilized onto the PCL surface and that the BMP-2/Hep-PCL fibers have more hydrophilic surface properties than PCL fibers alone. ALP activity, calcium deposition, and gene expression on BMP-2/Hep-PCL fibers showed significantly induced osteogenic differentiation relative to PCL fibers. Therefore, we suggest that BMP-2/Hep-PCL fibers have the potential to effectively induce osteogenic differentiation of PDLCs.

1. Introduction

Bone regeneration in alveolar bone defect/loss arising from inflammation, surgical resection, or trauma is important in periodontal tissue regeneration therapy and in pre-prosthetic, pre-implant surgery (Orciani et al., 2009; Wang et al., 2009). Many approaches have been developed to repair alveolar bone defect/loss, including autologous bone grafts, distraction osteogenesis, and guided bone regeneration (GBR) (Buser, Brägger, Lang, & Nyman, 1990; Chiapasco, Romeo, & Vogel, 2001; Cordaro, Amadé, & Cordaro, 2002; Schliephake, Neukam, & Wichmann, 1997). However, these methods have limitations such as extensive harvest of healthy tissue, intraoral distraction devices, and secondary infections.

Periodontal ligament cells (PDLCs), which display mesenchymal stem cell properties, are considered to be the key cell type involved in the regeneration of periodontal tissues. Recent studies demonstrated that PDLCs have the potential to differentiate into osteoblasts, chondrocytes and adipocytes (Gay, Chen, & MacDougall, 2007; Zhou et al., 2008). However, periodontal tissue regeneration using PDLCs alone requires a relatively long healing period.

Bone morphogenetic proteins (BMPs) belong to the transforming growth factor-β superfamily and are known as potential inducers of bone and cartilage regeneration. In addition to their role during tooth development, BMPs also play important roles in regulating morphogenesis and differentiation of many organs (Hogan, 1996; Wan & Cao, 2005; Xu et al., 2003; Yamashiro, Tummers, & Thesleff, 2003). Among the BMPs, BMP-2 has very strong osteoinductive properties. BMP-2 can improve gene expression during osteogenic differentiation *in vitro* including that of osteopontin, osteocalcin, bone sialoprotein, and alkaline phosphatase (Diefenderfer, Osyczka, Garino, & Leboy, 2003; Lecanda, Avioli, & Cheng, 1997). Recent studies reported that BMP-2 has the ability to stimulate the regeneration of bone and periodontal tissues *in vivo* (Jovanovic et al., 2003; Selvig, Sorensen, Wozney, & Wikesjö, 2002; Sorensen, Wikesjö, Kinoshita, & Wozney, 2004). Although BMP-2 and/or PDLCs have been successfully used to stimulate periodontal tissue regeneration, BMP-2 has a short half-life *in vivo*, and few studies have

* Corresponding author. Tel.: +82 2 958 9440; fax: +82 2 966 4572.
** Co-corresponding author. Tel.: +82 33 815 4604; fax: +82 33 255 7273.
E-mail addresses: kspark1223@kbsi.re.kr (K. Park), sjnb2@khu.ac.kr (B.-J. Choi).
[1] These authors contributed equally to this work.

0144-8617/$ – see front matter © 2013 Published by Elsevier Ltd.
http://dx.doi.org/10.1016/j.carbpol.2013.08.053

linked grafting of PDLCs with periodontal defects (Lang, Schüler, & Nolden, 1998; Nakahara et al., 2004; Sellers et al., 2000; vanDijk, Schakenraad, van der Voort, Herkströter, & Busscher, 1991).

To overcome these drawbacks, tissue engineering strategies have been suggested as an effective approach for regenerating periodontal tissue following alveolar bone defect/loss. Akizuki et al. (2005) and Hasegawa, Yamato, Kikuchi, Okano, and Ishikawa (2005) reported that PDLCs sheets can regenerate periodontal tissue and cementum in canine and rat models. BMP-2 loaded microspheres seeded with PDLCs have been shown to enhance periodontal healing and regeneration in animal models (Chen et al., 2005). Currently, nanofibrous scaffolds produced by an electrospinning process are being explored as scaffolds for tissue engineering. In addition, nanofibrous scaffolds can serve as suitable carriers to support initial cell adhesion similar to the extracellular matrix (ECM), and allow for diffusion of nutrients and metabolites during *in vitro* culture. Electrospun nanofiber poly(DL-lactide-co-glycolide, PLGA) scaffolds support PDLC adhesion, viability, and osteogenic differentiation (Inanç, Arslan, Seker, Elçin, & Elçin, 2009).

To facilitate bone tissue response to scaffolds, various growth factor delivery systems have been developed by modifying and functionalizing with polysaccharides. For example, in our previous studies, we developed a heparinized titanium implant to deliver growth factors directly to the implant site (Kim et al., 2011). Heparin has high binding affinity with growth factors (Sasisekharan, Ernst, & Venkataraman, 1997), and immobilization of heparin can minimize the rapid diffusion or release of proteins from substrates and improve the efficacy of proteins (Zhao et al., 2006; Bhakta et al., 2012).

Herein, we prepared fibrous scaffolds using polycarprolactone (PCL) as a carrier material for the proliferation and differentiation of PDLCs. PCL is a biodegradable and biocompatible polymer and is widely used in biomedical applications as a drug delivery carrier or scaffold for the proliferation and differentiation of a variety of cell types. Importantly, PCL has been approved by the Food and Drug Administration (FDA) (Ekaputra, Prestwich, Cool, & Hutmacher, 2011; Li et al., 2005; Porter, Henson, Ryan, & Popat, 2009). To effectively induce osteogenic differentiation, we functionalized the surface of PCL fibers with heparin and further immobilized them with BMP-2. We then characterized the functionalized PCL fibers and evaluated the release of BMP-2 from PCL fibers. Moreover, we investigated differentiation of PDLCs including cell proliferation, ALP activity, mineralization, and gene expression of osteocalcin and osteopontin.

2. Materials and methods

2.1. Materials

Heparin (average MW *ca.* 12,000 Da) was purchased from Pharmacia Hepar Co. (Franklin, OH). Polycarprolactone (PCL), dopamine hydrochloride, 1-ethyl-3-(3-dimethylaminopropyl)-carbodiimide (EDC) and N-hydroxysuccinimide (NHS) were obtained from Sigma Chemical Co. (St. Louis, MO). *Escherichia coli*-derived recombinant human bone morphogenetic protein-2 (BMP-2) was donated by Cowellmedi (Busan, Korea). Dulbecco's modified Eagle's medium (DMEM), fetal bovine serum (FBS), phosphate-buffered saline (PBS), and penicillin–streptomycin were purchased from Gibco-BRL (Rockville, MD, USA). The cell counting kit-8 (CCK-8) was purchased from Dojindo (Tokyo, Japan). BMP-2 ELISA kit was purchased from PeproTech Inc. (Rocky Hill, NJ, USA). All other chemicals were of the purest analytical grade available.

2.2. Cells isolation and culture

This study protocol was approved by the Institutional Review Board of Kyung Hee University Hospital at Gangdong (KHNMC MD IRB 2012-002). Periodontal ligament (PDL) tissues were obtained from premolar teeth extracted for orthodontic reasons. PDL tissues were dissected from the middle third of the root using a sterile scalpel blade, and the harvested PDL tissue was placed in a 4-cm-diameter culture plate. Tissues were left in the culture plate for 5–10 min and then the culture plate was flooded with complete medium (C-medium) [Dulbecco's modified Eagle's medium (DMEM) supplemented with 10% fetal bovine serum (FBS) and 1% antibiotics (penicillin 100 U/mM, streptomycin 0.1 mg/mL)]. The culture plate was kept in a humid incubator (37 °C with 5% CO_2). When the periodontal ligament cells (PDLCs) had grown to a confluence of approximately 70–80% (at 1×10^6 cells/mL), cells were detached using 0.05% trypsin-EDTA. PDLCs from passages 3 through 5 in a T-75 cm^2 flask were used.

2.3. Preparation of PCL fiber

PCL fibers were fabricated using the electrospinning method. In brief, PCL at a concentration of 20 wt% was dissolved in chloroform/DMF (2:1, v/v). The resulting solution was loaded into a 10 mL glass syringe equipped with an 18 gauge needle. The loaded syringe was placed in a syringe pump (KD-200, KD Scientific, Inc., USA). The distance between the syringe needle tip and collector was 10 cm, and the tip of the syringe was connected to the positive output of a high-voltage power supply (12 kV). The flow rate was set at 1 mL/h.

2.4. Flow cytometry

Adherent PDLCs were harvested in DMEM supplemented with 10% FBS and 1% antibiotics and resuspended at a concentration of 1×10^6 cells/mL in PBS with 5% FBS. Aliquots containing 1×10^6 cells were incubated with fluorescein isothiocyanate-conjugated mouse specific monoclonal antibodies (BD Biosciences, USA) directed against CD34, CD45, CD44, CD73, and CD90 for 30 min at room temperature (RT). Cells were washed three times in PBS solution with 5% FBS. Labeled cells were fixed in 1% formaldehyde in PBS prior to analysis using a FACs Calibur Cytometer (FC 500; Beckman Coulter, Fullerton, CA, USA).

2.5. Preparation of heparin-dopamine (Hep-DOPA) and surface modification of PCL fibers

To immobilize BMP-2 onto the surface of PCL fibers ($W \times L \times H = 1\ cm \times 1\ cm \times 0.01\ cm$), the surface of PCL fibers was modified with heparin-dopamine (Hep-DOPA). BMP-2 was subsequently immobilized onto the surface of the heparin-modified PCL fibers.

To functionalize and immobilize heparin to the surface of PCL fibers, heparin was conjugated with dopamine using EDAC (Lee, Yun, Park, & Kim, 2012). In brief, heparin (400 mg), EDAC (190.6 mg), and NHS (115 mg) were dissolved in 10 mL of MES buffer (pH 4.5) and allowed to react for 10 min. Dopamine hydrochloride (102.2 mg) dissolved in 1 mL of MES buffer (pH 4.5) was added to the heparin solution and allowed to react overnight. The mixture was dialyzed (MWCO 2000; spectrum®) against acidified distilled water for 2 days and lyophilized. The synthesis of Hep-DOPA was confirmed by ^1H NMR spectroscopy with the intrinsic peaks of dopamine appearing at 6.7–7.0 ppm. The number of dopamine molecules conjugated in each heparin chain was 4.6 ± 0.8.

To functionalize the surface of PCL fibers with highly negative-charged heparin, PCL fibers were immersed in a solution of

Hep-DOPA (2 mg/mL) dissolved in 10 mM Tris·HCl at pH 8.0, and gently shaken overnight in the dark. Heparin-modified PCL fibers (Hep-PCL) were washed with water and dried with N_2 gas. To quantify the immobilized amount of heparin on the PCL fibers, the toluidine blue method was used. Briefly, heparin-modified PCL (Hep/PCL) fibers were immersed in 1 mL of 0.2% (v/v) NaCl solution containing 1 mL of 0.005% (wt/v) toluidine blue solution. After gentle shaking for 30 min, 2 mL of hexane was added. Hep/PCL fibers were removed from the solution, and the absorbance of the aqueous phase was measured using a microplate reader (Bio-Rad, Hercules, CA, USA) at a wavelength of 620 nm. The amount of heparin from Hep/PCL fibers was calculated from a calibration curve that was constructed using various concentrations of heparin. The determined amount of heparin immobilized on the surface of PCL fibers was 10.2 ± 0.4 μg/sample.

To immobilize BMP-2 onto the surface of Hep-PCL fibers, BMP-2 at concentrations of 10 or 50 ng/mL was added to the Hep-PCL fibers immersed in 0.1 M MES buffer (pH 5.6) overnight with gentle shaking, then washed and dried.

2.6. Characterization of fibers

Surface morphologies of PCL, Hep-PCL, BMP-2 (10 ng)/Hep-PCL, and BMP-2 (50 ng)/Hep-PCL fibers were determined by scanning electron microscopy (SEM, S4800, Hitachi, Japan). Specimens were coated with gold using a sputter-coater (Eiko IB, Japan), and the SEM was operated at 3 kV. The surface composition of PCL, Hep-PCL, BMP-2 (10 ng)/Hep-PCL, and BMP-2 (50 ng)/Hep-PCL fibers were analyzed by X-ray photoelectron spectroscopy (XPS) on a K-alpha spectrometer (ESCALAB250 XPS System, Theta Probe AR-XPS System, Thermo Fisher Scientific, UK) with an Al Kα X-ray source (1486, 6 eV photons) at the Korea Basic Science Institute Busan Center. The C1s hydrocarbon peak at 284.84 eV was used as the reference for all binding energies. The area of each peak was normalized to the total peak area of all atomic elements to calculate surface atomic percentages. To confirm the hydrophilic properties of PCL and surface-modified PCL fibers, contact angles were measured with a goniometer (SEO Phoenix 300, Suwon, Korea). These experiments were repeated thrice.

2.7. In vitro BMP-2 release test

To evaluate the amount of BMP-2 released from BMP-2 (10 ng)/Hep-PCL fibers and BMP-2 (50 ng)/Hep-PCL fibers, each sample was soaked in a 50 mL conical tube (Falcon, USA) containing 1 mL PBS (pH 7.4) with gentle shaking at 100 rpm at 37 °C. At predetermined time intervals of 1, 3, 5, 10 h, and 1, 3, 5, 7, 14, 21, and 28 days, the supernatants were collected and replaced with fresh PBS solution. The amount of BMP-2 released was evaluated with an enzyme-linked immunosorbent assay (ELISA) kit according to the manufacturer's instructions using a microplate reader (Bio-Rad, Hercules, CA, USA) at 450 nm. This experiment was repeated thrice.

2.8. Cytotoxicity test

To evaluate the cytotoxicity of PCL fibers and surface-modified PCL fibers, we performed cytotoxicity tests according to the ISO/EN 10993 guidelines. PDLCs were seeded on 96-well plates at a concentration of 1×10^4 cells/well and incubated for 24 h at 37 °C with C-medium. PCL fibers and surface-modified PCL fibers were soaked in C-medium and incubated for 24 h at 37 °C. After 24 h of incubation, the C-medium in the PLDCs was aspirated, and PDLCs were washed with PBS and replaced with C-medium from the substrates. PDLCs were incubated for 48 h. At 24 and 48 h, the extraction medium was aspirated and CCK-8 proliferation kit (Dojindo, Japan) reagents were added to the PDLCs. PDLCs were then incubated for 1 h at 37 °C, and the optical density of live PDLCs was measured using a microplate reader at a wavelength of 450 nm. This experiment was repeated thrice.

2.9. F-actin staining

In order to observe the morphology of PDLCs grown on PCL, Hep-PCL, BMP-2 (10 ng)/Hep-PCL, and BMP-2 (50 ng)/Hep-PCL fibers, PDLCs were seeded at a concentration of 1×10^4 cells/cm^2 on the surface of substrates into a 24-well tissue-culture plate. After 24 h of incubation, the cells/substrates were rinsed with PBS and fixed in 3.7% formaldehyde for 30 min. After fixation, cells/substrates were immersed in a cytoskeleton buffer (5×10^{-3} M NaCl, 150×10^{-3} M $MgCl_2$, 5×10^{-4} M Tris–base and 0.5% triton X-100) for 5 min at 4 °C, followed by blocking buffer (5% FBS, 0.1% Tween-20 and 0.02% sodium azide in PBS) for 30 min at 37 °C. The cells/substrates were incubated with rhodamine-phalloidin (1:200) and DAPI (1:10,000). Substrates were mounted on microscope slides using mounting medium and observed by confocal laser scanning microscopy (LSM700, Zeiss, Germany).

2.10. PDLCs proliferation

PDLCs were seeded at a density of 1×10^5 cells/mL onto the surface of PCL, Hep-PCL, BMP-2 (10 ng)/Hep-PCL, and BMP-2 (50 ng)/Hep-PCL fibers in 24-well tissue-culture plates and maintained in C-medium. At 1, 3, and 7 days, substrates were rinsed with PBS and CCK-8 proliferation kit reagents were added to the substrates and were incubated for 1 h. Reagents were carefully transferred to 96-well plates. Optical density was measured using a microplate reader at a wavelength of 450 nm. This experiment was repeated thrice.

2.11. Alkaline phosphate (ALP) activity assay

To evaluate the early osteogenic differentiation of PDLCs, ALP activity was measured. In brief, cells were seeded at a density of 1×10^5 cells/mL on the surface of PCL, Hep-PCL, BMP-2 (10 ng)/Hep-PCL, and BMP-2 (50 ng)/Hep-PCL fibers in a 24-well tissue-culture plate and maintained in osteogenic medium (DMEM supplemented with 10% FBS, 50 μg/mL ascorbic acid, 10 nM dexamethasone, and 10 mM β-glycerophosphate in the presence of 100 U/mL penicillin and 100 μg/mL streptomycin) for 14 days. At predetermined time intervals of 3, 7, 10, and 14 days, PDLCs were washed with PBS, and 1X RIPA buffer was added to the cells. Cell lysates were centrifuged at 13,500 rpm at 4 °C for 3 min to remove cell debris. The supernatants were incubated with *p*-nitrophenyl phosphate solution for 30 min at 37 °C. The reaction was stopped by adding 500 μL of 1 N NaOH. ALP activity was determined by measuring the conversion of *p*-nitrophenyl phosphate to *p*-nitrophenol. Optical density was determined using a microplate reader at a wavelength of 405 nm. This experiment was repeated thrice.

2.12. Calcium deposition

To assess the late osteogenic differentiation, PDLCs were seeded at a density of 1×10^5 cells/mL on the surface of PCL and surface-modified PCL fibers in a 24-well tissue-culture plate and cultured in an osteogenic medium. At 21 days of culture, cells/substrates were washed with PBS, 0.5 N HCl was added to the cells/substrates, and PDLCs were harvested by centrifugation at 13,500 rpm for 1 min. The resulting supernatant was used for calcium deposition measurements using the QuantiChrom™ Calcium Assay Kit (DICA-500, BioAssay Systems, USA) according to the manufacturer's instructions. The amount of calcium produced was estimated by

Table 1
Surface elemental compositions of various PCL fibers.

Substrate	C%	N%	O%	S%
PCL	78.83 ± 0.98	1.00 ± 0.02	20.18 ± 1.00	–
Hep-PCL	73.43 ± 1.39	2.78 ± 0.26	21.77 ± 0.62	2.03 ± 0.49
BMP-2 (10 ng)/Hep-PCL	71.88 ± 1.57	4.02 ± 0.52	20.78 ± 0.33	3.32 ± 0.72
BMP-2 (50 ng)/Hep-PCL	70.61 ± 2.26	6.14 ± 0.63	20.00 ± 0.13	3.26 ± 1.50

measuring the absorbance at 612 nm using a microplate reader. This experiment was repeated thrice.

2.13. Quantitative real-time polymerase chain reaction (PCR)

The mRNA expression levels of osteogenic differentiation markers such as osteocalcin (OCN) and osteopontin (OPN) were investigated at 21 days by real-time PCR. In brief, 1×10^5 PDLCs were seeded on the surface of the PCL and surface-modified PCL fibers in a 24-well tissue-culture plate. After a 21-day incubation, cDNA was synthesized using the Superscript First-Strand Synthesis System (Invitrogen, Carlsbad, CA, USA) according to the manufacturer's instructions using 1 μg total RNA with oligo (dT). cDNA was amplified *via* PCR, using an RNA PCR kit (Bioneer Inc., Daejeon, South Korea), according to the manufacturer's instructions. The following oligonucleotide primers were used: OCN [(F) 5′-TGAGAGCCCTCACACTCCTC-3′, (R) 5′-ACCTTTGCTGGACTCTGCAC-3′], OPN [(F) 5′-GAGGGCTTGGTTGTCAGC-3′, (R) 5′-CAATTCTCATGGTAGTGAGTTTTCC-3′], GAPDH [(F) 5′-ACTTTGTCAAGCTCATTTCC-3′, (R) 5′-TGCAGCGAACTTTATTGATG-3′]. Real-time PCR reactions were performed with the above-mentioned specific primers. PCR amplification and detection were carried out on an ABI7300 Real-Time Thermal Cycler (Applied Biosystems, Foster, CA, USA) using the DyNAmo™ SYBR® Green qPCR Kit (Finnzymes, Espoo, Finland). The relative mRNA expression levels of OCN and OPN were normalized to GAPDH. This experiment was repeated thrice.

2.14. Statistical analysis

Quantitative data are presented as means ± standard deviation, and comparisons were carried out using one-way ANOVA (Systat Software, Inc., IL, USA). Differences were considered statistically significant at $^*P < 0.05$ and $^{**}P < 0.001$.

3. Results

3.1. Surface protein expression

To investigate stem cells using cell surface markers, flow cytometry was performed. The positive surface protein markers CD 90, CD73, and CD 44 were present in 95.8 ± 6.08%, 96.23 ± 3.78%, and 97.9 ± 3.64% of cells, respectively (Fig. 1). In contrast, the negative surface protein markers CD 34 and CD 45 were present in 0.06 ± 0.05% and 0% of cells, respectively.

3.2. Characterization of PCL and surface-modified PCL fibers

The surface morphologies of PCL, Hep-PCL, BMP-2 (10 ng)/Hep-PCL, and BMP-2 (50 ng)/Hep-PCL fibers were investigated by SEM. The surface of PCL fibers immobilized with heparin and BMP-2 showed a similar morphology to that of PCL fibers (Fig. 2A). To evaluate the elemental chemical compositions of PCL, Hep-PCL, BMP-2 (10 ng)/Hep-PCL, and BMP-2 (50 ng)/Hep-PCL fibers, an XPS analysis was conducted. The XPS wide-scan spectra of PCL, Hep-PCL, BMP-2 (10 ng)/Hep-PCL, and BMP-2 (50 ng)/Hep-PCL fibers and their corresponding surface elemental chemical compositions are shown in Fig. 2B and Table 1, respectively. Successful heparin modification on the surface of PCL fibers was confirmed by a increase of the O content from 20.18 ± 1.00% to 21.77 ± 0.62%, a increase of the S content from 0 to 2.03 ± 0.49%, and a increase of the N content from 1.00 ± 0.02% to 2.78 ± 0.26% compared to PCL fibers (Table 1). Moreover, successful immobilization of BMP-2 onto the surface of Hep-PCL fibers was confirmed by a decrease in the C content and increase in the N content compared to Hep-PCL fibers. The means ± standard deviation of the contact angle of PCL, Hep-PCL, BMP-2 (10 ng)/Hep-PCL, and BMP-2 (50 ng)/Hep-PCL fibers were 104.17 ± 4.9, 84.3 ± 6.4, 75.6 ± 7.6, 51.4 ± 21.8, respectively (Fig. 2C and Table 2). We also observed that PCL fibers containing BMP-2 were more hydrophilic than PCL fibers.

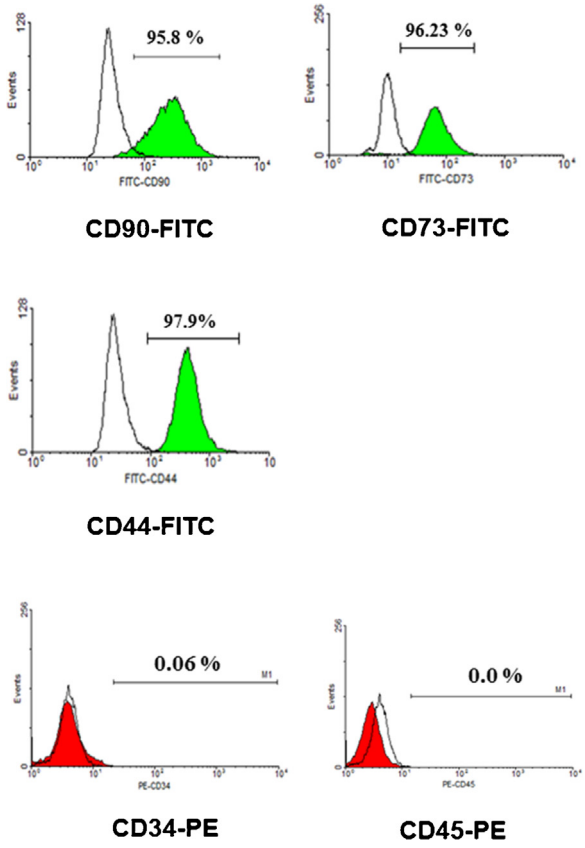

Fig. 1. Flow cytometry analysis of PDLCs labeled with CD 90, CD 73, CD 44, CD 34, and CD 45 antibodies (all antibodies with FITC conjugated).

Table 2
The mean ± standard deviation contact angle of PCL fibers and surface-modified PCL fibers.

Conditions	Contact angle (°)
PCL	104.17 ± 4.9
Hep-PCL	84.3 ± 6.4
BMP-2(10 ng)/Hep-PCL	75.6 ± 7.6
BMP-2(50 ng)/Hep-PCL	51.4 ± 21.8

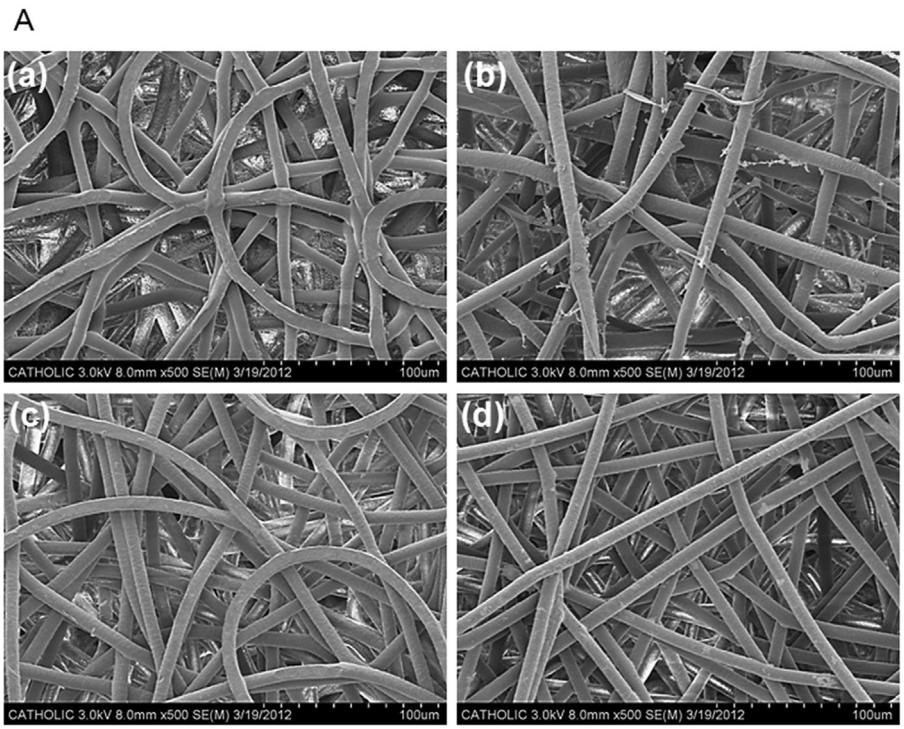

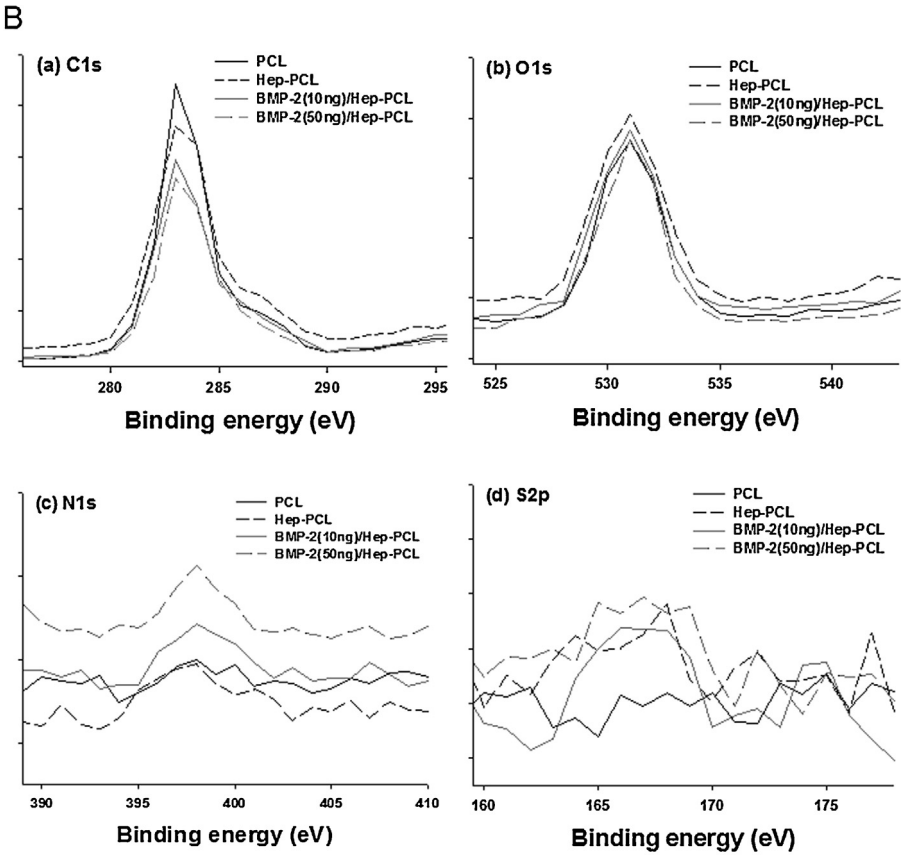

Fig. 2. (A) SEM images of PCL and surface-modified PCL fibers: (a) PCL, (b) Hep-PCL, (c) BMP-2 (10 ng)/Hep-PCL, and (d) BMP-2 (50 ng)/Hep-PCL fiber. (B) Representative XPS wide-spectra of PCL and surface-modified PCL fibers: (a) C1s, (b) O1s, (c) N1s and (d) S2p spectra. (C) Contact angles of PCL and surface-modified PCL fibers: (a) PCL, (b) Hep-PCL, (c) BMP-2 (10 ng)/Hep-PCL, and (d) BMP-2 (50 ng)/Hep-PCL fiber.

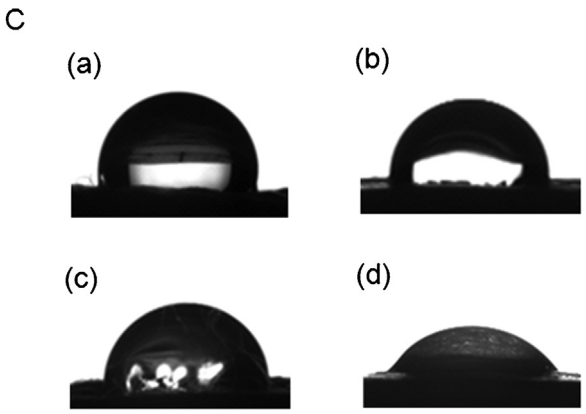

Fig. 2. (*Continued*).

3.3. In vitro BMP-2 release study

The BMP-2 release profiles of BMP-2 (10 ng)/Hep-PCL fibers and BMP-2 (50 ng)/Hep-PCL fibers are shown in Fig. 3. Over the 28-day study period, BMP-2 (10 ng)/Hep-PCL fibers and BMP-2 (50 ng)/Hep-PCL fibers exhibited sustained release. On day 1, 1.29 ± 0.82 ng and 1.98 ± 1.04 ng of BMP-2 was released from BMP-2 (10 ng)/Hep-PCL fibers and BMP-2 (50 ng)/Hep-PCL fibers, respectively. Over the 28-day study period, 3.74 ± 0.89 ng and 14.1 ± 0.82 ng of BMP-2 was released from BMP-2 (10 ng)/Hep-PCL fibers and BMP-2 (50 ng)/Hep-PCL fibers, respectively.

3.4. Cytotoxicity test and F-actin staining

Cytotoxicity tests for PCL, Hep-PCL, BMP-2 (10 ng)/Hep-PCL and BMP-2 (50 ng)/Hep-PCL fibers were performed using PDLCs (Fig. 4A). Cell viability in all groups was maintained above 98% compared to that in control group after a 48-h incubation time. No significant cytotoxic effects were observed during incubation periods of up to 48 h. The adhesion of PDLCs was observed after seeding PDLCs onto the surface of PCL, Hep-PCL, BMP-2 (10 ng)/Hep-PCL and BMP-2 (50 ng)/Hep-PCL fibers, by performing F-actin staining. More adhesion was observed in PDLCs seeded onto the surface of PCL fibers containing BMP-2 than for PDLCs seeded onto the surface of PCL fibers (Fig. 4B).

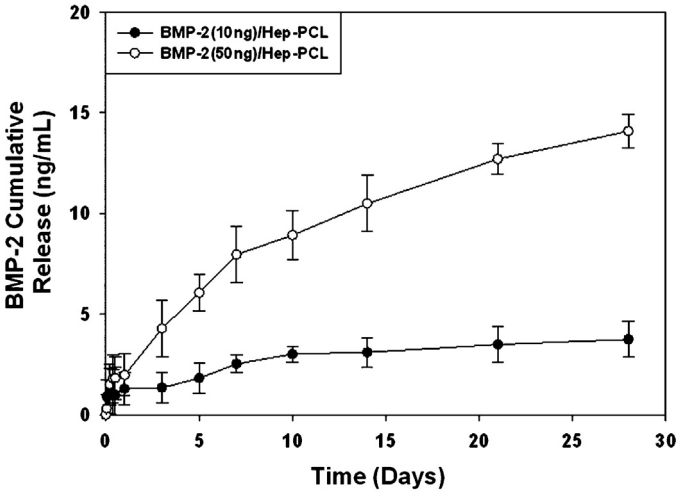

Fig. 3. Cumulative release profiles of BMP-2 from BMP-2 (10 ng)/Hep-PCL (●) and BMP-2 (50 ng)/Hep-PCL fiber (○). The error bars represent mean ± SD ($n = 5$). These experiments were repeated thrice.

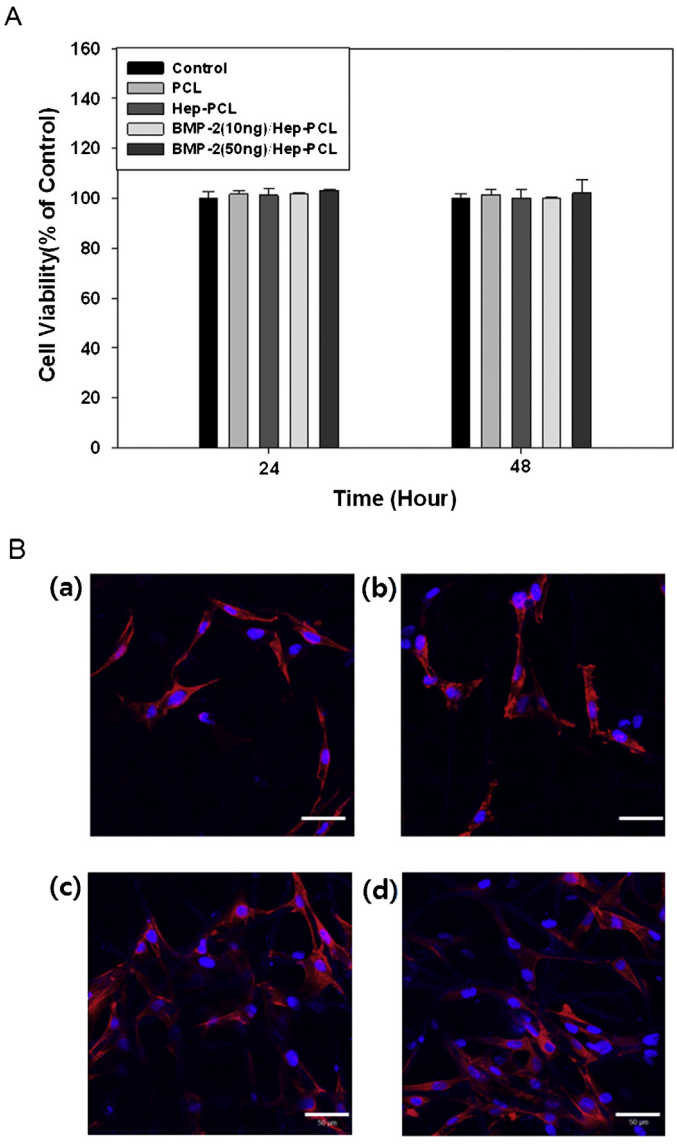

Fig. 4. (A) Cytotoxicity test of PCL, Hep-PCL, BMP-2 (10 ng)/Hep-PCL, and BMP-2 (50 ng)/Hep-PCL fibers against periodontal ligament cells (PDLCs). (B) Morphologies of PDLCs cultured on (a) PCL, (b) Hep-PCL, (c) BMP-2 (10 ng)/Hep-PCL, and (d) BMP-2 (50 ng)/Hep-PCL fibers for 1 day.

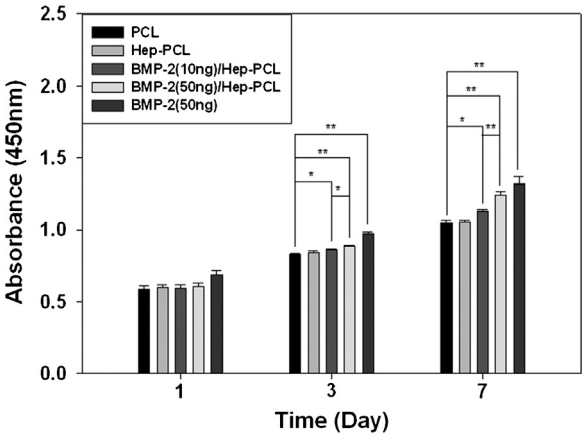

Fig. 5. Cell proliferation of PDLCs grown on PCL, Hep-PCL, BMP-2 (10 ng)/Hep-PCL, and BMP-2 (50 ng)/Hep-PCL fibers against PDLCs after 1, 3, and 7 day incubation. The error bars represent mean ± SD ($n = 5$). These experiments were repeated thrice ($^{*}P < 0.05$ and $^{**}P < 0.001$).

3.5. Cell proliferation

PDLC proliferation on PCL, Hep-PCL, BMP-2 (10 ng)/Hep-PCL and BMP-2 (50 ng)/Hep-PCL fibers was evaluated. PDLC proliferation gradually increased in all groups throughout the incubation period, up to 7 days (Fig. 5). At 1 day, there were no significant differences in PDLC proliferation between any of the groups. There were significant differences in PDLC proliferation between PDLCs grown on PCL fibers containing BMP-2 and those grown on PCL fibers ($^{*}P < 0.05$ and $^{**}P < 0.001$) at 3 and 7 days of culture. Moreover, there were significant differences in PDLC proliferation between the PDLCs cultured on BMP-2 (10 ng)/Hep-PCL fibers and those cultured on BMP-2 (50 ng)/Hep-PCL fibers at 3 and 7 days ($^{*}P < 0.05$).

3.6. Osteogenic differentiation of PDLCs

We evaluated ALP activity as a marker of early osteogenic differentiation at 3, 7, 10, and 14 days (Fig. 6A). At 3 days, there were no significant differences in ALP activity among all groups. At 7 days, ALP activity of PDLCs in PCL fiber containing BMP-2 group was higher compared to that of PDLCs in PCL fiber group, but the difference was not statistically significant. At 10 and 14 days, ALP activity was significantly different between PDLCs in the PCL fiber-containing BMP-2 group and the PCL fiber group ($^{*}P < 0.05$ and $^{**}P < 0.001$). Furthermore, the ALP activity of PDLCs between the BMP-2 (10 ng)/Hep-PCL fiber group and the BMP-2 (50 ng)/Hep-PCL fiber group was significantly different at 10 and 14 days ($^{*}P < 0.05$). After treating with noggin as a BMP-2 inhibitor, ALP activities of PDLCs grown on two BMP-2/Hep-PCL fibers were markedly increased compared to those on PCL and Hep-PCL fiber groups (see Supporting Information, Fig. S1) suggesting that osteogenic differentiation of PDLCs is mainly due to the released BMP-2 from PCL fibers, not from cells.

To investigate the late osteogenic differentiation, the amount of calcium deposited on PCL, Hep-PCL, BMP-2 (10 ng)/Hep-PCL and BMP-2 (50 ng)/Hep-PCL fibers after culturing PDLCs for 21 days was determined (Fig. 6B). There was a statistically significant difference in the amount of calcium deposited on PDLCs between the PCL fiber containing BMP-2 groups and the PCL fiber group ($^{*}P < 0.05$). Additionally, calcium deposition on PDLCs grown on BMP-2 (10 ng)/Hep-PCL fibers was significantly greater than that in PDLCs grown on BMP-2 (50 ng)/Hep-PCL fibers ($^{*}P < 0.05$). To evaluate the mRNA expression levels of OCN and OPN for osteogenic differentiation of PDLCs cultivated in all groups, we conducted real-time PCR after incubation for 21 days. OCN and OPN expression levels in PDLCs grown on BMP-2 (10 ng)/Hep-PCL fibers were significantly higher than those in PDLCs grown on PCL fibers ($^{*}P < 0.05$) (Fig. 6C-a and b). Also, OCN and OPN expression levels in PDLCs grown on BMP-2 (50 ng)/Hep-PCL fibers were markedly higher than those in PDLCs grown on PCL fibers ($^{**}P < 0.001$). Furthermore, OCN and OPN expression levels in PDLCs cultivated on BMP-2 (50 ng)/Hep-PCL fibers were significantly higher compared to those in PDLCs cultivated on BMP-2 (10 ng)/Hep-PCL fibers ($^{*}P < 0.05$).

4. Discussion

Periodontal ligament (PDL), alveolar bone and cementum are important tooth-supporting tissues. PDL defects from inflammation, if left untreated, can lead to the loosening and subsequent loss of teeth. PDLCs, with their strong proliferation and differentiation potential in the periodontium, play a key role in the regeneration of periodontal defects. Although the use of PDLCs in the regeneration of PDL defects has many advantages, there are also some problems associated with their use such as the insufficient availability of cells, the difficulty in harvesting them, and time-consuming cell culture. Because of these problems for clinical treatments, we prepared BMP-2-delivering heparinized PCL (BMP-2/Hep-PCL) fibers *via* the successive immobilization of heparin-dopamine and BMP-2 on the surface of PCL fibers for enhancing proliferation and osteogenic differentiation of PDLCs.

We synthesized a heparin-dopamine (Hep-DOPA) conjugate by a 1-ethyl-3-dimethylaminopropyl carbodiimide (EDC)-mediated reaction between the carboxylic groups of heparin and the amine groups of dopamine so as to immobilize heparin onto the surface of PCL fibers. As previously reported, this is a very simple method to immobilize heparin onto the surface of substrates (Lee et al., 2012) because the ortho-dihydroxyphenyl (catechol) functional group in dopamine can form strong covalent and noncovalent bonds with inorganic, organic, and metallic materials (Fan, Lin, Dalsin, & Messersmith, 2005; Lee, Dellatore, Miller, & Messersmith, 2007; Lee, Scherer, & Messersmith, 2006). BMP-2 was subsequently immobilized onto the surface of Hep-PCL fibers *via* electrostatic interactions between positively charged BMP-2 and negatively charged heparin. After the sequential immobilization of heparin and BMP-2 on the surface of PCL fibers, the characterization of PCL and surface-functionalized PCL fibers was confirmed with XPS and contact angle measurement. Following the immobilization of Hep-DOPA, N and S contents increased on the surface of Hep-PCL fibers compared to PCL fibers. Moreover, after the immobilization of BMP-2 onto the surface of Hep-PCL fibers, the N content increased, whereas the C and O contents decreased compared to that in the Hep-PCL fibers, indicating that BMP-2 was successfully immobilized onto the surface of Hep-PCL fibers. The BMP-2 immobilized Hep-PCL fiber surfaces showed a significantly smaller water contact angle than that of the PCL fiber surfaces, indicating that the Hep-PCL fiber surface with immobilization of BMP-2 was more hydrophilic compared to the PCL fiber surface. Previous studies reported that BMP-2 immobilized carboxymethyl chitosan (CMCS)-grafted Ti surface or heparin-grafted Ti surface were more hydrophilic than pristine Ti (Shi, Neoh, Kang, Poh, & Wang, 2009a, 2009b).

BMP-2 is known as one of the most potent osteoinductive growth factors. It has been used for the treatment of spinal fusion and bone fracture healing (De Biase & Capanna, 2005; Westerhuis, van Bezooijen, & Kloen, 2005). Although BMP-2 has been commercially available for use in clinical treatments, there are limitations to its use due to requirement for large doses of BMP-2 (2.1–12 mg), its short half-life *in vivo*, and its side effects such as immune response and bone over-growth from the defect site due to its rapid diffusion in large amounts (Gautschi, Frey, & Zellweger, 2007; Shields et al., 2006). To date, various biomaterials, including collagen

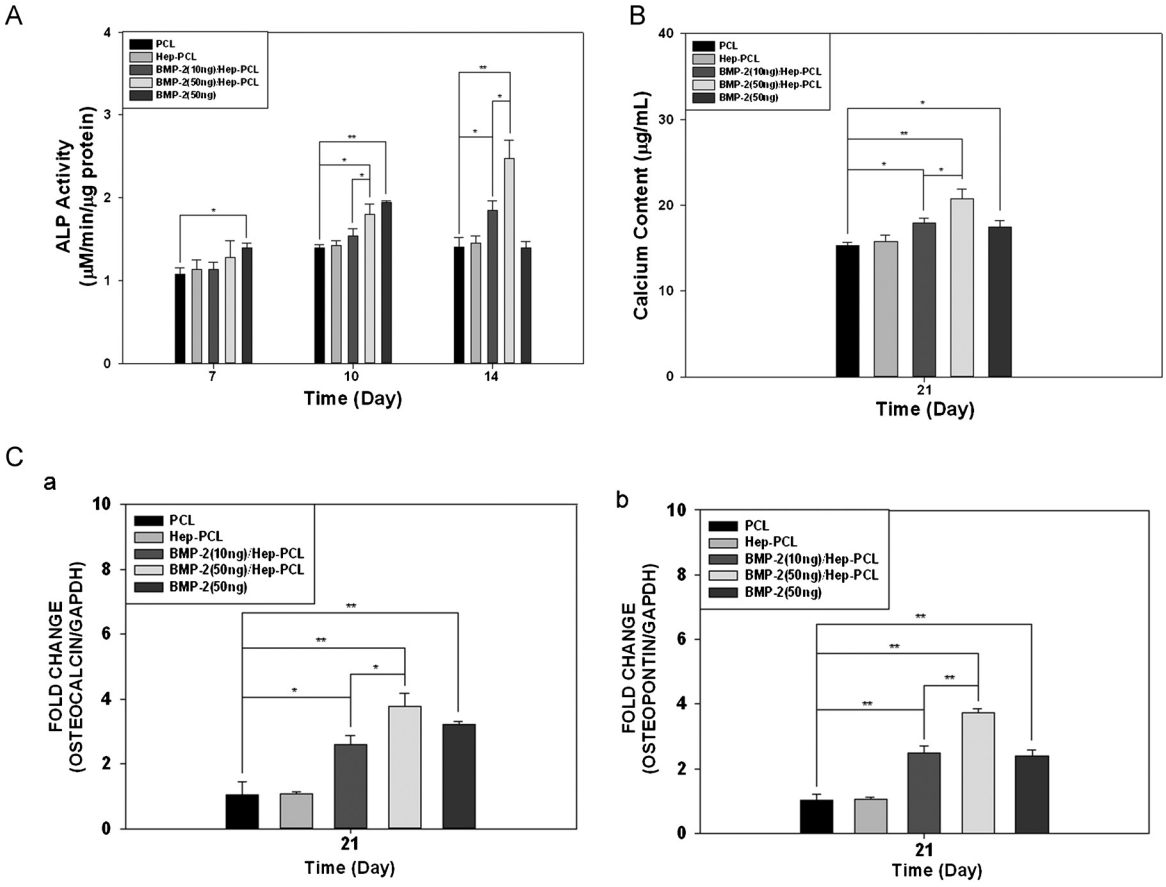

Fig. 6. (A) ALP activity of PDLCs grown on PCL, Hep-PCL, BMP-2 (10 ng)/Hep-PCL, and BMP-2 (50 ng)/Hep-PCL fibers against PDLCs after 3, 7, 10, and 14 day incubation. (B) Calcium deposition of PDLCs grown on PCL, BMP-2 (10 ng)/Hep-PCL, and BMP-2 (50 ng)/Hep-PCL fibers against PDLCs after 21 day incubation. (C) Real-time PCR analysis of gene expressions of (a) osteocalcin and (b) osteopontin of PDLCs grown on PCL, BMP-2 (10 ng)/Hep-PCL, and BMP-2 (50 ng)/Hep-PCL fibers against PDLCs after 21 day incubation. The error bars represent mean ± SD ($n = 5$). These experiments were repeated thrice ($^{*}P < 0.05$ and $^{**}P < 0.001$).

gels, sponges, hyaluronic acid, dextran, chitosan, poly (lactic-co-glycolic) acid, and fibrin scaffolds have been used as BMP-2 delivery systems (Chua, Neoh, & Kang, 2008; Kim et al., 2007; King, King, Cruchley, Wozney, & Hughes, 1997; Lee, Ho, et al., 2006; Shen, Hu, Yang, Bei, & Wang, 2009; Shi, Neoh, Kang, Poh, & Wang, 2009a, 2009b). However, some of these BMP-2 delivery systems exhibit problems such as uncontrolled release rates, rapid release of BMP-2, and high initial burst releases (Jeon et al., 2008). We overcame these problems with the addition of heparin. Heparin, which is composed of many sulfate and carboxyl groups, is known to have high binding affinities for various growth factors and the ability to regulate the release of growth factors (Ishibe et al., 2009; Kim et al., 2011; Park et al., 2008; Sasisekharan et al., 1997). In our release study, we observed a sustained release of BMP-2 with no high initial burst release pattern of BMP-2, which may be due to the strong electrostatic interactions between the highly negatively charged heparin and the highly positively charged BMP-2. These data support our previous study in which we showed that Hep-DOPA grafted titanium (Hep-Ti) substrates allowed for sustained release of BMP-2 and gentamicin (Lee et al., 2012).

We evaluated PDL cell proliferation on all substrates and found that it increased in a time-dependent manner. Additionally, PDL cell proliferation on BMP-2/Hep-PCL fibers increased significantly compared to that on PCL fibers at days 3 and 7. These results indicated that BMP-2 has a definite effect on PDL cell proliferation; this result is consistent with a report from Park et al. (2006). However, other studies demonstrated that cell proliferation on rhBMP-2 immobilized Ti substrates did not show a significant increase compared to that on pristine Ti discs (Kim et al., 2011; Shi, Neoh, Kang, Poh, & Wang, 2009a, 2009b). Therefore, the effect of BMP-2 on cell proliferation is still under debate.

To understand the osteogenic differentiation of PDLCs on all substrates, we evaluated ALP activity and calcium deposition. ALP activity and calcium deposition are widely used as markers for early and late differentiation of osteoblast-like cells, respectively (Turksen, Bhargava, Moe, & Aubin, 1992; van den Beucken et al., 2006). ALP activity of PDLCs cultured on all substrates was increased by the released BMP-2 from BMP-2/Hep-PCL fibers in a time-dependent manner. There was no significant difference in the ALP activity of PDLCs grown on PCL fibers and those grown on BMP-2/Hep-PCL fibers at days 3 and 7. In contrast, there was a significant difference in the ALP activity of PDLCs grown on PCL fibers and those grown on BMP-2/Hep-PCL fibers after 10 days or 14 days of culture. The ALP activity of PDLCs cultured on BMP-2 (50 ng)/Hep-PCL fibers was significantly higher than that in those cultured on BMP-2 (10 ng)/Hep-PCL fibers after 10 days or 14 days of culture. As expected from the ALP activity data, the amount of calcium deposition on PDLCs grown on BMP-2/Hep-PCL fibers was significantly higher than that on PDLCs grown on PCL fibers. Kim et al. (2011) reported that the ALP activity and the amount of calcium deposited on MG-63 cells cultured on BMP-2-immobilized Ti surface were significantly different as compared to those on MG-63 cells cultured on pristine Ti. Taken together, these results indicate that BMP-2 stimulates osteogenic differentiation of PDLCs.

We evaluated the induction of osteogenic differentiation of PDLCs on all substrates by measuring gene expression levels

of osteocalcin and osteopontin. It has been reported that the expression of osteocalcin and osteopontin as markers of osteoblast differentiation is upregulated after osteoblast differentiation (Diefenderfer et al., 2003; Lecanda et al., 1997). mRNA expression levels of osteocalcin and osteopontin in PDLCs grown on BMP-2/Hep-PCL fibers were markedly increased as compared to those in PDLCs grown on PCL fibers. These results indicated that BMP-2/Hep-PCL substrates directly enhanced the osteogenic differentiation of PDLCs. The effects of BMP-2/Hep-PCL substrates on osteogenic differentiation of PDLCs were significantly greater than those seen on PCL substrates. In particular, the BMP-2 (50 ng)/Hep-PCL substrates showed significantly enhanced osteogenic differentiation of PDLCs compared to that of the PCL and BMP-2 (10 ng)/Hep-PCL substrates.

We found that use of BMP-2/Hep-PCL substrates was an effective option for the regeneration of periodontal defects. To achieve more conclusive outcomes for periodontal therapy, further *in vivo* studies are needed to optimize dose levels and to determine the best mechanism to control the release of BMP-2.

5. Conclusions

In the present study, we successfully immobilized BMP-2 onto the surface of heparinized PCL fibers to prepare BMP-2/Hep-PCL fibers. The BMP-2/Hep-PCL fibers showed sustained BMP-2 release profiles over 28 days with no cytotoxicity against periodontal ligament cells (PDLCs). We showed that BMP-2/Hep-PCL fibers significantly induced osteogenic differentiation of PDLCs with a significant increase in ALP activity and calcium deposition compared to that in PCL fibers. In addition, BMP-2/Hep-PCL substrates effectively induced osteogenic differentiation of PDLCs with a significant increase in the mRNA expression levels of osteocalcin and osteopontin. Therefore, we suggest that BMP-2/Hep-PCL fibers can induce the osteogenic differentiation of PDLCs. However, further *in vivo* evaluations are required to optimize the dose of BMP-2 and the efficacy of BMP-2/Hep-PCL fibers to achieve more conclusive outcomes for the clinical use of BMP-2/Hep-PCL fibers in the regeneration of periodontal defects.

Acknowledgments

This study was supported by a grant from the Korea Healthcare Technology R&D Project, Ministry of Health & Welfare, Republic of Korea (HI11C0388) and a KBSI grant (T33513) to KP.

Appendix A. Supplementary data

Supplementary data associated with this article can be found, in the online version, at http://dx.doi.org/10.1016/j.carbpol.2013.08.053.

References

Akizuki, T., Oda, S., Komaki, M., Tsuchioka, H., Kawakatsu, N., Kikuchi, A., et al. (2005). Application of periodontal ligament cell sheet for periodontal regeneration: A pilot study in beagle dogs. *Journal of Periodontal Research*, *40*, 245–251.

Bhakta, G., Rai, B., Lim, Z. X., Hui, J. H., Stein, G. S., van Wijnen, A. J., et al. (2012). Hyaluronic acid-based hydrogels functionalized with heparin that support controlled release of bioactive BMP-2. *Biomaterials*, *33*, 6113–6122.

Buser, D., Brägger, U., Lang, N. P., & Nyman, S. (1990). Regeneration and enlargement of jaw bone using guided tissue regeneration. *Clinical Oral Implants Research*, *1*, 22–32.

Chen, F., Wu, Z., Wang, Q., Wu, H., Zhang, Y., Nie, X., et al. (2005). Preparation and biological characteristics of recombinant human bone morphogenetic protein-2-loaded dextran-co-gelatin hydrogel microspheres, in vitro and in vivo studies. *Pharmacology*, *75*, 133–144.

Chiapasco, M., Romeo, E., & Vogel, G. (2001). Vertical distraction osteogenesis of edentulous ridges for improvement of oral implant positioning: A clinical report of preliminary results. *International Journal of Oral and Maxillofacial Implants*, *16*, 43–51.

Chua, P. H., Neoh, K. G., Kang, E. T., & Wang, W. (2008). Surface functionalization of titanium with hyaluronic acid/chitosan polyelectrolyte multilayers and RGD for promoting osteoblast functions and inhibiting bacterial adhesion. *Biomaterials*, *29*, 1412–1421.

Cordaro, L., Amadé, D. S., & Cordaro, M. (2002). Clinical results of alveolar ridge augmentation with mandibular block bone grafts in partially edentulous patients prior to implant placement. *Clinical Oral Implants Research*, *13*, 103–111.

De Biase, P., & Capanna, R. (2005). Clinical applications of BMPs. *Injury*, *36*, S43–S44.

Diefenderfer, D. L., Osyczka, A. M., Garino, J. P., & Leboy, P. S. (2003). Regulation of BMP-induced transcription in cultured human bone marrow stromal cells. *Journal of Bone and Joint Surgery*, *85*, 19–28.

Ekaputra, A. K., Prestwich, G. D., Cool, S. M., & Hutmacher, D. W. (2011). The three-dimensional vascularization of growth factor-releasing hybrid scaffold of poly (ε-caprolactone)/collagen fibers and hyaluronic acid hydrogel. *Biomaterials*, *32*, 8108–8117.

Fan, X., Lin, L., Dalsin, J. L., & Messersmith, P. B. (2005). Biomimetic anchor for surface-initiated polymerization from metal substrates. *Journal of the American Chemical Society*, *127*, 15843–15847.

Gautschi, O. P., Frey, S. P., & Zellweger, R. (2007). Bone morphogenetic proteins in clinical applications. *ANZ Journal of Surgery*, *77*, 626–631.

Gay, I. C., Chen, S., & MacDougall, M. (2007). Isolation and characterization of multipotent human periodontal ligament stem cells. *Orthodontics and Craniofacial Research*, *10*, 149–160.

Hasegawa, M., Yamato, M., Kikuchi, A., Okano, T., & Ishikawa, I. (2005). Human periodontal ligament cell sheets can regenerate periodontal ligament tissue in an athymic rat model. *Tissue Engineering*, *11*, 469–478.

Hogan, B. L. (1996). Bone morphogenetic proteins in development. *Current Opinion in Genetics and Development*, *6*, 432–438.

Inanç, B., Arslan, Y. E., Seker, S., Elçin, A. E., & Elçin, Y. M. (2009). Periodontal ligament cellular structures engineered with electrospunpoly(DL-lactide-co-glycolide) nanofibrous membrane scaffolds. *Journal of Biomedical Materials Research Part A*, *90*, 186–195.

Ishibe, T., Goto, T., Kodama, T., Miyazaki, T., Kobayashi, S., & Takahashi, T. (2009). Bone formation on apatite-coated titanium with incorporated BMP-2/heparin in vivo. *Oral Surgery, Oral Medicine, Oral Pathology, Oral Radiology and Endodontics*, *108*, 867–875.

Jeon, O., Song, S. J., Yang, H. S., Bhang, S. H., Kang, S. W., Sung, M. A., et al. (2008). Long-term delivery enhances in vivo osteogenic efficacy of bone morphogenetic protein-2 compared to short-term delivery. *Biochemical and Biophysical Research Communications*, *369*, 774–780.

Jovanovic, S. A., Hunt, D. R., Bernard, G. W., Spiekermann, H., Nishimura, R., Wozney, J. M., et al. (2003). Long-term functional loading of dental implants in rhBMP-2 induced bone. A histologic study in the canine ridge augmentation model. *Clinical Oral Implants Research*, *14*, 793–803.

Kim, J., Kim, I. S., Cho, T. H., Lee, K. B., Hwang, S. J., Tae, G., et al. (2007). Bone regeneration using hyaluronic acid-based hydrogel with bone morphogenic protein-2 and human mesenchymal stem cells. *Biomaterials*, *28*, 1830–1837.

Kim, S. E., Song, S. H., Yun, Y. P., Choi, B. J., Kwon, I. K., Bae, M. S., et al. (2011). The effect of immobilization of heparin and bone morphogenic protein-2 (BMP-2) to titanium surfaces on inflammation and osteoblast function. *Biomaterials*, *32*, 366–373.

King, G. N., King, N., Cruchley, A. T., Wozney, J. M., & Hughes, F. J. (1997). Recombinant human bone morphogenetic protein-2 promotes wound healing in rat periodontal fenestration defects. *Journal of Dental Research*, *76*, 1460–1470.

Lang, H., Schüler, N., & Nolden, R. (1998). Attachment formation following replantation of cultured cells into periodontal defects–a study in minipigs. *Journal of Dental Research*, *77*, 393–405.

Lecanda, F., Avioli, L. V., & Cheng, S. L. (1997). Regulation of bone matrix protein expression and induction of differentiation of human osteoblasts and human bone marrow stromal cells by bone morphogenetic protein-2. *Journal of Cellular Biochemistry*, *67*, 386–396.

Lee, D. W., Yun, Y. P., Park, K., & Kim, S. E. (2012). Gentamicin and bone morphogenic protein-2 (BMP-2)-delivering heparinized-titanium implant with enhanced antibacterial activity and osteointegration. *Bone*, *50*, 974–982.

Lee, H., Dellatore, S. M., Miller, W. M., & Messersmith, P. B. (2007). Mussel-inspired surface chemistry for multifunctional coatings. *Science*, *318*, 426–430.

Lee, H., Scherer, N. F., & Messersmith, P. B. (2006). Single-molecule mechanics of mussel adhesion. *Proceedings of the National Academy of Sciences of the United States of America*, *103*, 12999–13003.

Lee, T. C., Ho, J. T., Hung, K. S., Chen, W. F., Chung, Y. H., & Yang, Y. L. (2006). Bone morphogenetic protein gene therapy using a fibrin scaffold for a rabbit spinal-fusion experiment. *Neurosurgery*, *58*, 373–380.

Li, W. J., Tuli, R., Okafor, C., Derfoul, A., Danielson, K. G., Hall, D. J., et al. (2005). A three-dimensional nanofibrous scaffold for cartilage tissue engineering using human mesenchymal stem cells. *Biomaterials*, *26*, 599–609.

Nakahara, T., Nakamura, T., Kobayashi, E., Kuremoto, K., Matsuno, T., Tabata, Y., et al. (2004). In situ tissue engineering of periodontal tissues by seeding with periodontal ligament-derived cells. *Tissue Engineering*, *10*, 537–544.

Orciani, M., Trubiani, O., Vignini, A., Mattioli-Belmonte, M., Di Primio, R., & Salvolini, E. (2009). Nitric oxide production during the osteogenic differentiation of human periodontal ligament mesenchymal stem cells. *Acta Histochemica*, *111*, 15–24.

Park, J. S., Park, K., Woo, D. G., Yang, H. N., Chung, H. M., & Park, K. H. (2008). Triple constructs consisting of nanoparticles and microspheres for bone-marrow-derived stromal-cell-delivery microscaffolds. *Small*, *4*, 1950–1955.

Park, Y. J., Kim, K. H., Lee, J. Y., Ku, Y., Lee, S. J., Min, B. M., et al. (2006). Immobilization of bone morphogenetic protein-2 on a nanofibrous chitosan membrane for enhanced guided bone regeneration. *Biotechnology and Applied Biochemistry*, *43*, 17–24.

Porter, J. R., Henson, A., Ryan, S., & Popat, K. C. (2009). Biocompatibility and mesenchymal stem cell response to poly(epsilon-caprolactone) nanowire surfaces for orthopedic tissue engineering. *Tissue Engineering, Parts A*, *15*, 2547–2559.

Sasisekharan, R., Ernst, S., & Venkataraman, G. (1997). On the regulation of fibroblast growth factor activity by heparin-like glycosaminoglycans. *Angiogenesis*, *1*, 45–54.

Schliephake, H., Neukam, F. W., & Wichmann, M. (1997). Survival analysis of endosseous implants in bone grafts used for the treatment of severe alveolar ridge atrophy. *Journal of Oral and Maxillofacial Surgery*, *55*, 1227–1233.

Sellers, R. S., Zhang, R., Glasson, S. S., Kim, H. D., Peluso, D., D'Augusta, D. A., et al. (2000). Repair of articular cartilage defects one year after treatment with recombinant human bone morphogenetic protein-2 (rhBMP-2). *Journal of Bone and Joint Surgery*, *82*, 151–160.

Selvig, K. A., Sorensen, R. G., Wozney, J. M., & Wikesjö, U. M. (2002). Bone repair following recombinant human bone morphogenetic protein-2 stimulated periodontal regeneration. *Journal of Periodontology*, *73*, 1020–1029.

Shen, H., Hu, X., Yang, F., Bei, J., & Wang, S. (2009). The bioactivity of rhBMP-2 immobilized poly(lactide-co-glycolide) scaffolds. *Biomaterials*, *30*, 3150–3157.

Shields, L. B., Raque, G. H., Glassman, S. D., Campbell, M., Vitaz, T., Harpring, J., et al. (2006). Adverse effects associated with high-dose recombinant human bone morphogenetic protein-2 use in anterior cervical spine fusion. *Spine*, *31*, 542–547.

Shi, Z., Neoh, K. G., Kang, E. T., Poh, C. K., & Wang, W. (2009). Surface functionalization of titanium with carboxymethyl chitosan and immobilized bone morphogenetic protein-2 for enhanced osseointegration. *Biomacromolecules*, *10*, 1603–1611.

Shi, Z., Neoh, K. G., Kang, E. T., Poh, C., & Wang, W. (2009). Titanium with surface-grafted dextran and immobilized bone morphogenetic protein-2 for inhibition of bacterial adhesion and enhancement of osteoblast functions. *Tissue Engineering, Parts A*, *15*, 417–426.

Sorensen, R. G., Wikesjö, U. M., Kinoshita, A., & Wozney, J. M. (2004). Periodontal repair in dogs: Evaluation of a bioresorbable calcium phosphate cement (Ceredex) as a carrier for rhBMP-2. *Journal of Clinical Periodontology*, *31*, 796–804.

Turksen, K., Bhargava, U., Moe, H. K., & Aubin, J. E. (1992). Isolation of monoclonal antibodies recognizing rat bone-associated molecules in vitro and in vivo. *Journal of Histochemistry and Cytochemistry*, *40*, 1339–1352.

van den Beucken, J. J., Walboomers, X. F., Boerman, O. C., Vos, M. R., Sommerdijk, N. A., Hayakawa, T., et al. (2006). Functionalization of multilayered DNA-coatings with bone morphogenetic protein 2. *Journal of Controlled Release*, *113*, 63–72.

vanDijk, L. J., Schakenraad, J. M., van der Voort, H. M., Herkströter, F. M., & Busscher, H. J. (1991). Cell-seeding of periodontal ligament fibroblasts.A novel technique to create new attachment. A pilot study. *Journal of Clinical Periodontology*, *18*, 196–199.

Wan, M., & Cao, X. (2005). BMP signaling in skeletal development. *Biochemical and Biophysical Research Communications*, *328*, 651–657.

Wang, S., Zhang, Z., Zhao, J., Zhang, X., Sun, X., Xia, L., et al. (2009). Vertical alveolar ridge augmentation with beta-tricalcium phosphate and autologous osteoblasts in canine mandible. *Biomaterials*, *30*, 2489–2498.

Westerhuis, R. J., van Bezooijen, R. L., & Kloen, P. (2005). Use of bone morphogenetic proteins in traumatology. *Injury*, *36*, 1405–1412.

Xu, X., Jeong, L., Han, J., Ito, Y., Bringas, P., Jr., & Chai, Y. (2003). Developmental expression of Smad1-7 suggests critical function of TGF-beta/BMP signaling in regulating epithelial-mesenchymal interaction during tooth morphogenesis. *International Journal of Developmental Biology*, *47*, 31–39.

Yamashiro, T., Tummers, M., & Thesleff, I. (2003). Expression of bone morphogenetic proteins and Msx genes during root formation. *Journal of Dental Research*, *82*, 172–176.

Zhao, B., Katagiri, T., Toyoda, H., Takada, T., Fukuda, T., Chung, U. I., et al. (2006). Heparin potentiates the in vivo ectopic bone formation induced by bone morphogenic-2. *Journal of Biological Chemistry*, *281*, 23246–23253.

Zhou, Y., Hutmacher, D. W., Sae-Lim, V., Zhou, Z., Woodruff, M., & Lim, T. M. (2008). Osteogenic and adipogenic induction potential of human periodontal cells. *Journal of Periodontology*, *79*, 525–534.